



NONISOTHERMAL SIMULATION OF ELECTRODEPOSITION

Tahseen A. Al-Hattab
Alhatab.1@gmail.com

Sata K. Ajjam
Satajam58@yahoo.com

University of Babylon- College of Engineering-Electrochemical Engineering Department

ABSTRACT

The simulation of electrochemical deposition is developed by using a non-isothermal model. The model consists of two parts; the first is a continuum part that simulates the transport of heat and mass and the voltage distributions, and the second is a stochastic noncontinuum part that simulates the bulk diffusion, surface diffusion, and adsorption of the particles. The finite element method is used to solve the differential-algebraic governing equations of the continuum part whereas the Kinetic Monte Carlo method is used to simulate the particle actions in the non-continuum part. The model is applied to the electrodeposition of Zn in ZnSO₄ additive-free electrolyte. A comparison is made between the experimental and the simulated results including the surface morphology and the temperature distributions. The results indicated that the simulation model is very promising to be used for such a complicated process.

Keywords: Thermal simulation, electrodeposition, modeling, Mote-Carlo method

NOMENCLATURE

Symbol	Description	Unit
C	concentration	mol/l
C _a	anion concentration	mol/l
C _c	cation concentration	mol/l
C _p	heat capacity	J/mol K
D _b	bulk solution diffusion coefficient	m ² /s
D _s	surface diffusion coefficient	m ² /s
E	activation energy	J/mol
E	electrical field	V/m
e _{z_a} e _{z_c}	anion, caion electric charge	C
F	Faraday constant	96485 C/mol
F	FE force vector	
F	FE system matrix	
J	Jacobian matrix	
K	FE stiffness matrix	
k	thermal conductivity	W/m.K
Σ	Metal-specific conductance	S/m
l	length of a unit cell	m
N	number of neighbors particles	
Q	Ohmic heat generation	W/m ³
R	molar gas constant	J/mol K
s	interface position	m

Symbole	Description	Unit
T	temperature	K
t	time	s
V_{el}	volume of the electrolyte	m^3
\mathbf{z}	FE variables vector	
z	distance from surface	M
	Greek symbols	
ϵ	dielectric permittivity	F/m
θ	site occupation probability	
Λ	equivalent conductance	$m^2S/mole$
ν	frequency of an action	
ρ	density	kg/m^3
Φ	applied voltage	V
ΔH	heat of formation	J/kg

INTRODUCTION

Recent research efforts have found some success in the simulation of electrochemical metal deposition. Such processes involve heterogeneous and homogeneous reactions that occur among the species including charges that are moved by diffusion, convection, and migration. In order to control the quality of the products produced by this technique of deposition, several parameters must be studied and evaluated to achieve the deposited properties and growth morphology. In general, the modeling and the simulation of the electrodeposition process are divided into two different scale phenomena, the macroscopic (continuum) phenomenon and the microscopic discrete (noncontinuum) one. The continuum phenomenon involves the mass, fluid, and heat transfer whereas the noncontinuum phenomenon consists of surface nucleation, metal deposition, and adsorption of metal ions. Different methods were used to solve the models of the continuum phenomena such as Finite Elements Methods (FEM), Finite Differences Methods (FDM), and Finite Volumes Methods (FVM). On the other hand, and depending on the point of modeling view, many stochastic techniques were used to simulate the noncontinuum phenomenon, however, the most interesting technique is the Kinetic Monte Carlo (KMC) method (Kalos et al., 1986). Although the continuum and the noncontinuum models diverge in the length scale, the time scale is different. There is a large difference between the fast local stochastic events and the slow variations that occur at longer scales on the field of the transport phenomena. The challenge of simulating coupled dynamic processes that span wide ranges of time and length scales is of broad interest. Multiscale methods are now beginning to emerge to provide a systematic and correct connection between events at different scales. External code linkage has been performed recently in a variety of applications such as unimolecular surface reaction (Vlachos, 1997) and metal film growth (Hansen et al., 2000). Different simulations based on MC methods have been developed to examine the electrodeposition process at the microscopic level. Some of these works were focused on individual steps of the overall reaction mechanism, rather than on the overall mechanism that consists of a variety of steps and pathways (Kalos et al., 1986), (Allen, and Tildesley, 1990), (Alkire, and Braatz, 2004). Many researchers studied experimentally the importance of surface diffusion in the electrodeposition process (Mehl, and Bockris, 1957), (Bockris, and Enyo, 1962), (Hillson, 1954). They supported this importance whereas other workers (Vitanov et al., 1974), (Ogata et al., 1982), (Hurlen, 1993) favored the mechanism of metal adsorption and incorporation at the kink. Although it was (Slaiman Q. J. M. and W. J. Lorenz, 1974) suggested that surface diffusion plays a role only at very low overpotentials, the

testing of such a hypothesis requires more investigations and evaluations of the effect of each parameter that controls the electrodeposition process (Alkire, 2003). On the other hand, some of the experimental works evaluated the effect of temperature on the kinetics parameters of the electrodeposition process (Jingxian et al., 2003) and the effect of heat dissipated during the metal deposition on the flow field of the electrolyte (Schroter et al., 2002). A code is required for each scale. External linkage of the multiscale codes is desirable since improvements can then be made in a component code at one scale without affecting the codes at other scales. Different algorithms (Ismail et al., 2003), (Gear, and Kevrekidis, 2003), (Lopez et al., 2002) have been performed recently to reduce the computation time of the simulation at each scale. Recently, a multiscale electrodeposition simulation (Pricer et al. 2002) was carried out using a three-dimensional (KMC) noncontinuum model linked to a one-dimensional continuum finite differences diffusion model. The assumption of isothermal stagnant electrolyte was considered in the work. The electrodeposition of copper in copper sulfate electrolyte was simulated and compared with the experimental results under constant potential. They focused their attention on the noncontinuum model and the reactions near the surface rather than the transport phenomena of the mass and the heat through the electrolyte. The simulation of electrodeposition onto resistive substrates was done (Tobias, and Wijnsman, 1953), (Alkire, 1971), (Matlosz et al. 1992) by combining the microscopic MC non continuum model with the continuum model based on the macroscopic resistance model that considers the current-voltage distribution as the main key of the model. These models were coupled (Drews et al, 2005) to form the multiscale model used for the simulation of copper electrodeposition. The resistance model did not consider the governing equations of the fluid mass and heat transfer associated with the deposition process. Generally, most of the simulation and the experimental works were concentrated on the electrodeposition of copper in different electrolyte conditions. However, in the previous works, the simulation of the electrochemical deposition was carried out based on the assumption of an isothermal process with no variation in temperature during the deposition, and all the parameters and the properties were taken at a constant temperature. The novel feature of the present work is a nonisothermal simulation method for metal electrodeposition. The applicability of the model is evaluated by the simulation of the deposition of Zinc in an additive-free electrolyte. A nonisothermal macroscopic model is used to simulate the continuum model. The effect of concentration-temperature-voltage distributions on stochastic microscopic events is considered. The finite element method is used to solve the system of the governing equation of the continuum model. A multiscale generic model is used to link the stochastic MC electrodeposition with the 2-D FE code. The simulation results are compared with the experimental results to check the validity of the present model.

MATHEMATICAL MODEL

The simulation of the electrochemical process consisted of two parts namely; the continuum and the non-continuum parts. The details of the two parts are described as follows:

Continuum part

In order to describe the continuum model that is used in this work, it is essential to describe the governing equations that control the transport phenomena in the electrochemical deposition of metal ions in a cell consisting of two electrodes immersed in an electrolytic solution. The mass and the heat transfer associated with the voltage distribution are described as follows:

The differential equations that describe the transfer of the cations toward the cathode and the transfer of anions toward the anode are as follows:

Mass transfer

$$\frac{\partial C_{\alpha}}{\partial t} = -\nabla \cdot (-D_{\alpha} \nabla C_{\alpha} + \mu_{\alpha} E C_{\alpha} + u C_{\alpha}) \quad (1)$$

$$\alpha = c, a$$

where α represents either the subscripts (c) and (a) which denote the cation and the anion respectively.

The above equation represents the combination of three effects on the concentration of both ions; which are mass diffusion, electric field, and the flow of the electrolyte, where (u) is the electrolyte velocity determined via the solution of the Navier-Stoke equation. According to Fick's law, (D) is the diffusion coefficient of the cations and the anions, whereas (μ) is the charge mobility of both ions. (E) is the electrical field along the electrolyte related to ions concentrations via the Poisson equation.

Voltage Distribution

$$\nabla \cdot E = -\nabla^2 \Phi = -e(z_c C_c - z_a C_a) / \epsilon \quad (2)$$

where (Φ) is the applied potential, (ez_c) and (ez_a) are the cations and anions electric charges respectively, and (ϵ) is the dielectric permittivity of the electrolyte. The problem of electrochemical deposition involves considering the heat transfer in a domain consisting of two distinct subdomains, electrolyte (Ω_e) and metal (Ω_m), where ($\Omega_e + \Omega_m = \Omega$). The differential equations governing the heat transfer can be written as follows:

Heat transfer:

$$\rho_e c_e \frac{\partial T_e}{\partial t} = k_e \nabla^2 T_e - u \cdot \nabla T_e + \rho_e g + Q_e^S \quad \text{in } \Omega_e \quad (3)$$

and

$$\rho_m c_m \frac{\partial T_m}{\partial t} = k_m \nabla^2 T_m + Q_m^S \quad \text{in } \Omega_m \quad (4)$$

where the subscripts (e) and (m) denote the electrolyte and the metal (solid) respectively, (Q^S) is the Ohmic heat generated due to the flow of electrical current through both the electrolyte and the metals of electrodes and the deposited particles.

$$Q_m^S = \Phi^2 (\sigma l) / V_{el} \quad \text{and} \quad Q_e^S = \Phi^2 (\Lambda C l) / V_{el}$$

where (σ) is the specific conductance of the metal, (Λ) is the equivalent conductance of the electrolyte, (l) is the specific length used here as the length of the unit cell, and (V_{el}) is the volume of the electrolyte. The complete description of the heat transfer problem involves the definition of the conditions at the interface boundary (Γ_{em}) where the phase change occurs, are:

$$\begin{aligned} T_{em} &= T_f \\ -k_m \frac{\partial T_m}{\partial n} &= -k_e \frac{\partial T_e}{\partial n} + \rho(-\Delta H_f) \frac{\partial S}{\partial t} \quad \text{on } \Gamma_{em} \end{aligned} \quad (5)$$

where (S) represents the position of the interface,

$\left(\frac{\partial S}{\partial t}\right)$ the interface velocity, and (T_f) is the temperature at the interface. In this part, the above continuum model is applied to a thin layer (2D) electrolyte that exists in an electrochemical cell. In such a case the effect of natural convection on the velocity-pressure fields can be neglected. Moreover, with the absence of external mixing, it is fearful enough to assume that the electrolyte is a stagnant liquid. This means that the heat transfer is controlled only by conduction. The system of the nonlinear partial differential equations and the algebraic equations (1-5) was solved by the finite element method. The implicit finite difference method was used to discretize the time derivative in the partial differential equation whereas Galerkin's method was used to obtain the finite element equations. The discretization scheme leads to a system of nonlinear algebraic equations described as follows:

$$F(z) = (C + \frac{1}{2} \Delta t K) z^{t+\Delta t} - (C - \frac{1}{2} \Delta t K) z^t - \frac{1}{2} \Delta t (f^{t+\Delta t} - f^t) = 0 \quad (6)$$

with a vector (z) contains cation concentrations (C) , the temperatures (T) and the overpotentials (Φ) ,

$$z = (C_1, \dots, C_N, T_1, \dots, T_N, \Phi_1, \dots, \Phi_N)^T$$

and a vector function (F) with components

$$F = (F(C_1), \dots, F(C_N), F(T_1), \dots, F(T_N), F(\Phi_1), \dots, F(\Phi_N))^T.$$

The Newton method was used to solve the nonlinear equation (6).

$$z^{n+1} = z^n - J(z)^{-1} F(z) \quad (7)$$

The linearized equations were described by the Jacobian matrix (J) , which is determined by numerical differentiation,

$$(J(z))_{ij} = \frac{(F_i(z + \Delta z_j) - F_i(z))}{\Delta z_j} + O(\Delta z_j) \quad (8)$$

In order to achieve global convergence of solutions, a simple line search strategy is employed in the Newton method. Initial guesses for the solution can be found from the solution of the last time step which usually gives good initial guesses as long as the time step size is not large.

Non-continuum part

This part represents the stochastic simulation of electrodeposition of metal which is carried out by the Kinetic Monte Carlo (KMC) algorithm. The simulation region was represented by a 2-D grid (matrix) where the cathode and the anode are located at the center and at the boundaries of the region respectively. The ions in the simulation were represented by squares in the grid and considered pseudo particles moved and deposited in the cell. The simulation model was carried out with a grid of 960x960 units and about 1.5×10^8 as a maximum number of particles. At each time step, each particle can only make one movement. The movements are a function of the location, the temperature, and the voltage at that location. Three types of possible movements can be made by the particle; bulk diffusion, surface diffusion, and adsorption. The algorithm used to simulate the KMC model can be described as follows:

Select randomly a particle site (location, k), and depending on the occupation (θ_k) different movements are attempted. If $(\theta_k=0)$, only adsorption is attempted while if $(\theta_k=1,6)$ different movements are proposed; bulk diffusion and surface diffusion, see Figure(1). The rate of each movement is computed based on the frequency and the probability of the movement. The frequency (ν) for a particle to diffuse from one site to another was proposed based on the expression $(\nu = ND_p / l^2)$ (Gomer,1990) whereas the frequency for movement of a

particle at the metal surface (surface diffusion) was determined according to the expression ($v = ND_s e^{\Delta E / kT} / l^2$) (Levi, and Kotrola, 1997). The reaction mechanism, as well as the adsorption, are modeled in this work by using one-step Arrhenius and Tafel kinetics

$$(v = N\kappa_s e^{\Delta E / kT - zF\Phi / RT} / l) \quad (\text{Rikvold et al., 2004})$$

The Monte Carlo time step (t_{MC}) is selected to be the smallest inverse of the frequencies.

$$t_{MC} = \text{Min}(v_1, v_2, \dots, v_J) \quad (9)$$

where (J) is the number of actions for each particle.

At each time step, the particles perform different actions according to the KMC model, and the configuration of the deposited material is changed.

Simulation procedure

Figure (2) shows the schematic diagram of the procedure used in this work to simulate the electrodeposition process of Zinc in the additive-free (Zn_2SO_4) electrolyte. In every simulated time step the non-continuum KMC part is executed in order to determine the deposition of the metal and the change in the surface morphology based on the concentration-temperature-voltage distributions which were already estimated from the continuum part. This will take about (4×10^3) KMC steps. In this work, it is found that the Monte Carlo time step (t_{MC}) was about 2.6×10^{-7} seconds in the real-time of the experimental electrodeposition process. Later the continuum part was executed for the new configuration of the metal surface and then the concentration-temperature-voltage distributions were evaluated. The sequence was repeated for the whole computation time. The code of the simulation program was written with VB6 for irregular grids of more than (5000) triangular elements shown in Figure (3). The computer program consists of four parts; the main program and three other subprograms. The computation procedure of the computer program can be summarized as follows: The main program, NIECDS, executes the code that starts and controls other subprograms. ContFEM subprogram runs the code for solving the continuum model using the finite element method to determine the distributions of the temperature, concentration, and voltage throughout both the electrolyte and the deposited metal region. The results are sent to the NIECDS program. The non-Cont KMC subprogram runs the code of stochastic simulation of the noncontinuum model. Based on the data received from the NIECDS program the surface morphology is updated during a period of time that is explicitly limited to 0.01 seconds. The results then return to the NIECDS program. The results data at each time step are stored and plotted using the PltSav subprogram. ASCII type files are used to save these data whereas the images of the surface morphology and the distribution of temperature, concentration, and voltage are saved as image types. Simulation work was run on a PC with a 3.2 GHz Core2Duo processor and 2Gbyte RAM.

EXPERIMENTAL WORK.

The validity of the model proposed in this work is checked against the results of an experimental program performed in this work. The electrodeposition of zinc metal in an additive-free electrolyte of (0.2N) $ZnSO_4$ was used in this work. The applied voltage used was between (10-30) volts. Figure (4) shows the electrochemical cell and other accessories which are used in this work. The cell (10x10cm) is constructed from Perspex and covered with a foil of polyethylene to minimize the heat lost from the cell. The cathode is made as a thin disc of 1cm diameter and 2mm thickness, whereas the anode is made as a wire of 1mm diameter supported at the boundaries of the cell. However, the cell is made to satisfy the assumption of a two-dimension problem. Fifteen type-K thermocouples were inserted at the bottom of the cell to measure the temperature field. The thermocouples are connected to a data acquisition

(DAQ) hardware that is supported by compatible software which is used to store the values of the temperatures during the experiment time. Figure (5) shows the grids of the thermocouples attached to the bottom of the cell. A digital camera is connected to the computer. It is used to capture and then transfer the images of the cell during the electrodeposition of the materials. The capture mode of the camera used in this work is 20 frames per second with a resolution of 3648x2736 pixels for the captured image. A computer program working online is used to analyze the captured images. It is designed to extract the change in the deposited metal and then determine the average radius and the rate of deposition during the experiment. For any experiment, the first captured image is used as a base one and the later images are compared with it. The difference between the base and any image at a certain time will produce the amount of metal deposited at that time. This technique is used in the software, image analysis, which is designed to monitor and capture 20fps images of the propagation of metal deposition during the experiments. The software which is built with visual basic code is always taking into account the noise of the image colors by using different colored filters to enhance the analysis of the image.

RESULTS AND DISCUSSION

The results obtained in the present work will be presented and discussed in this section. The morphologies created by the simulation models developed in this work are discussed. Figure (6) shows typical simulated results of the isothermal and non-isothermal models compared with the experimental results at an applied voltage of (20) Volts. Based on a visual inspection, there are some differences between both simulated images and the experimental images. First of all, it is clear that the simulated images indicate that the aggregate of the non-isothermal simulation is denser than that of the isothermal simulation. Furthermore, the comparison indicates that the radius of the solid-liquid interface for the non-isothermal simulation is closer to the experimental deposition compared to the isothermal simulation during the time of the experiments. Moreover, the isothermal simulation needed more time to accomplish the same value of the radius. It is also observed that the symmetry of the deposition for the non-isothermal simulation is better than the symmetry for the isothermal simulation. However, a quantitative analysis of the images is needed for the evaluation of the simulation of the electrodeposition process based on both the isothermal and the non-isothermal models. Figure (7) shows the isotherm of temperature during the experiment's time for deposition of Zn at an applied voltage of 20 volts. Due to the shortage of the measured values of temperature, only the upper half section of the cell is analyzed and plotted. However, as a result of the growing deposit, the Ohmic heat generated within the solid materials leads to an increase in the region's temperature wherever the metal exists. Although heat is generated within the electrolyte, it is still less than the heat generated within the deposited metal. As a rough evaluation, the measured temperatures are less than the simulated. The over-estimated values of temperature may be due to the assumption of insulated upper and lower surfaces of the cell which is proposed in the present mathematical model. Actually, there is an amount of heat lost from the surfaces of the cell. These amounts of heat losses increase with time and with the increase in the applied voltage. Even so, the differences between the experimental results and the simulated results are acceptable if it is compared with the complexity of the problem. The average temperature is now calculated to study how the step-change in temperature moves with time as a thermal wave.

$$T_{av}(t) = \frac{\int_{A(r_{max}(t))} \rho c_P T dA}{\int_{A(r_{max}(t))} \rho c_P dA}.$$

Note that the average temperature is always based on the area of the deposited metal.

Figure (8) shows the change in average temperature for the deposited zinc with time for different values of applied voltage. As the deposition of metal proceeds, the density of the deposited metal through the area of deposition decreases. Even though the average temperature increases with time. The decrease in the density of the deposited metal means that the ratio of the amount of the solid materials to the liquid decreases too. The temperatures of the solid materials are higher than that of the liquid this means that the average temperature in the region of less density is lower than that of higher density. Therefore, the amount of heat generated within the area of the deposited metal increases the average temperature of both metal and electrolyte around the deposited region. As the applied voltage increase from (10V) to (30V) the average temperature increases from (301K) to (318K) for the first (300) seconds compared with the simulated values of (302K) and (321K) for at the same period. It is found that the electrolyte reaches the boiling temperature for long-term deposition under high applied voltage. Figure. (9) shows the gradual effect of the applied voltage on the rate of deposition during the time of the experiments. In general, the rate of deposition undergoes a high fluctuation around an average value that increases with time. This is of course due to the random nature of the problem. The results also show that the order of magnitude of the rate of deposition increases with the increase in the applied voltage. With the aid of the expression of Arrhenius - Tafel kinetics, it is possible to expect how the rate of the deposition is affected by the change in the value of the applied voltage. As a comparison between the experimental results of the rate of deposition and the simulated results based on both the isothermal and the non-isothermal models, it is found that the difference between simulated results are small and are close to the experimental results except for high applied voltage. At a high value of applied voltage, the increase in material temperature accelerates the deposition process and then increases its rate. Figure (10) shows the effect of applied voltage on the average radius of the deposition area. The average radius is determined as the average sum of the maximum radius measured relative to the center of the cathode all over the region of the deposited metal

$$R_{av} = \frac{I}{M} \sum_i^M \text{Max}(R_i(\vartheta)) \quad \dots\dots\vartheta \in (0, 2\pi).$$

It is found that the radii predicted by the non-isothermal model are closer to those measured experimentally, especially at the high value of the applied voltage where the effect of temperature acts as the controlling factor of the deposition process. This is due to the sensitivity of the diffusion and the adsorption of particles to the increase in temperature during the electrodeposition process. The comparison between the simulation prediction and the experimental results indicates that the isothermal simulation gives an unacceptable prediction for the average radius of the deposited metal compared with the results of the non-isothermal simulation. At applied voltage (15V) the nonisothermal simulation predicted an average radius of about (21mm) at the time (500s) compared with the experimental value of (22mm) at the same time, whereas the isothermal simulation predicted the average radius as (18mm) at the same time and applied voltage. However, It is clearly found that the difference between the nonisothermal and the isothermal simulations increases as both times and the applied voltage increase.

CONCLUSIONS

In this work, a nonisothermal simulation model is proposed for electrochemical deposition. The model consists of a continuum part that included the macroscopic behavior of heat-mass transfer with voltage distribution within the electrochemical cell. In this model, the Ohmic heat generated within the deposited metal and the electrolyte is taken into account in addition to the heat of metal formation. The second part of the model includes the microscopic non continuum stochastic behavior which describes the movement of the molecules such as bulk

and surface diffusion and the adsorption on the metal surface. The model is applied to the electrodeposition of Zinc in an additive-free Zn_2SO_4 solution. The comparison between the experimental results and the numerical simulation was done. It is found that the temperature variations have a significant effect on controlling the electrodeposition process, especially at the advanced time of the deposition process. The bulk and the surface diffusion and adsorption action of the particles are affected by temperature. Therefore, the simulation of such a process will involve errors if it is assumed as an isothermal process. It is also found that the prediction of metal surface morphology and the extent of the metal-electrolyte interface is closer to the experimental results when the simulation is based on the nonisothermal model rather than the isothermal model. Most of the computation time was spent in the simulation of the non-continuum stochastic part. The effect of temperature on the adsorption and the diffusion rates controls the movements of the simulated particles and accelerates the electrodeposition rate in an exponential manner. It is believed that the present work represents a more realistic simulation model for electrochemical deposition than other similar models, especially for the metal of high Ohmic resistance.

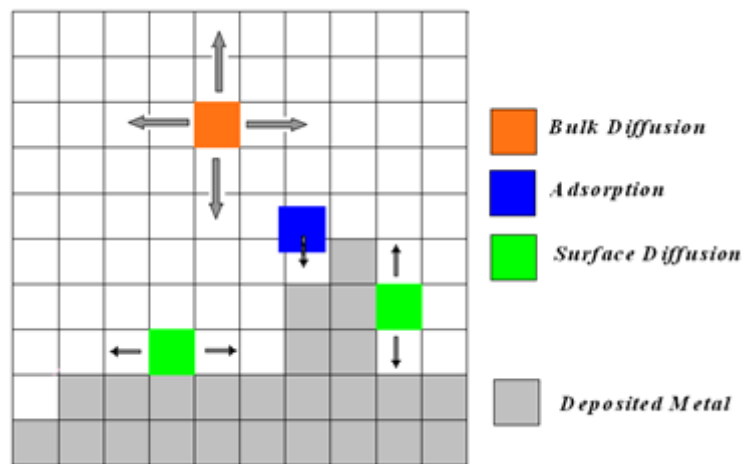


Fig. 1. Types of hypothetical particle movements

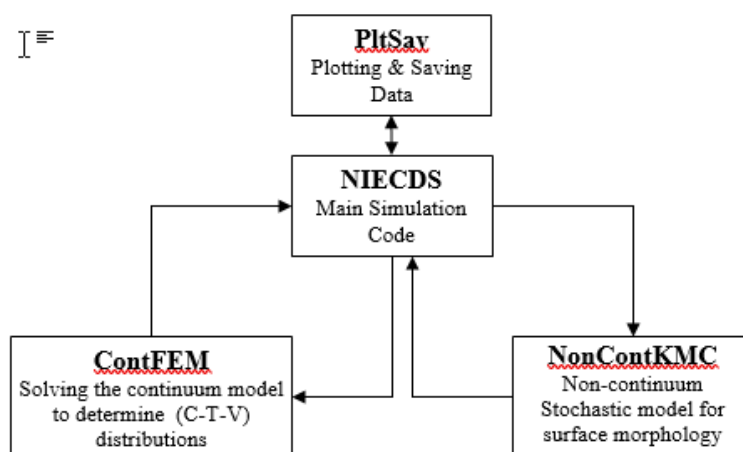


Fig. 2. Block diagram of the simulation procedure

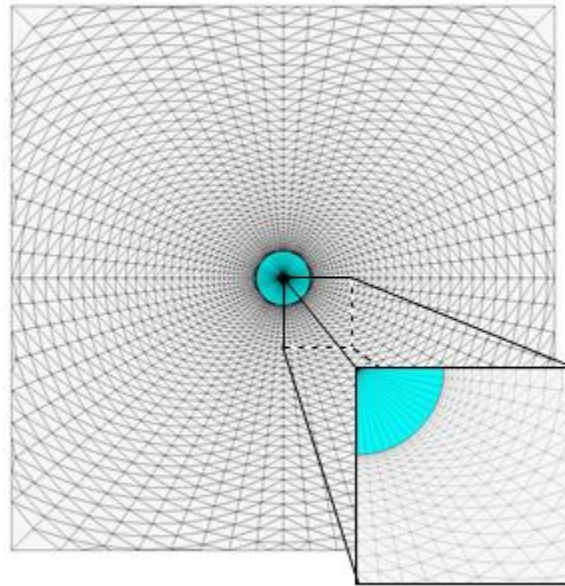


Fig. 3. 2-D grid of the computational continuum domain

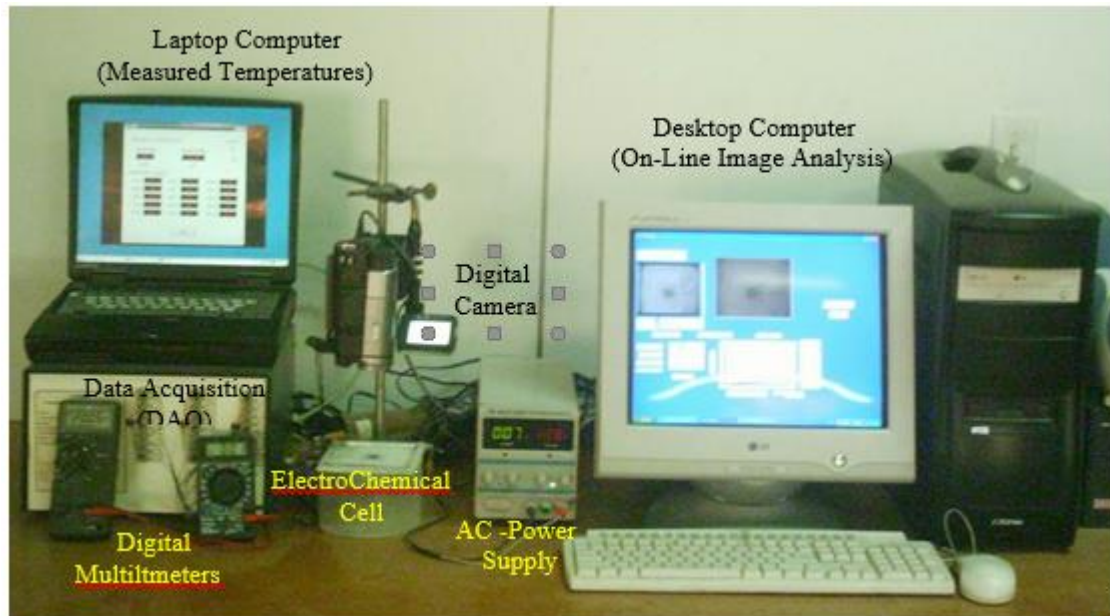


Fig. 4. Experimental setup of measuring system used in this work.

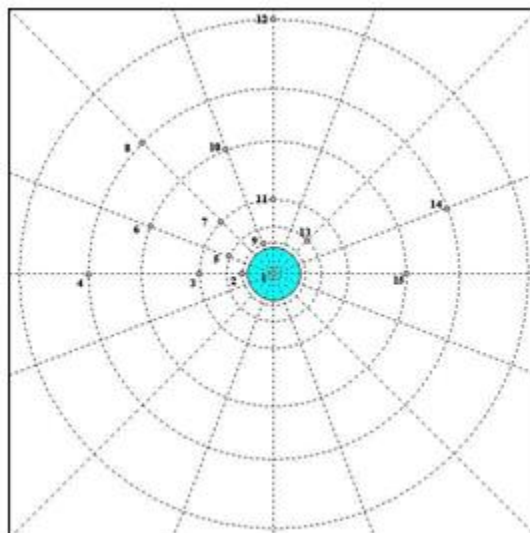
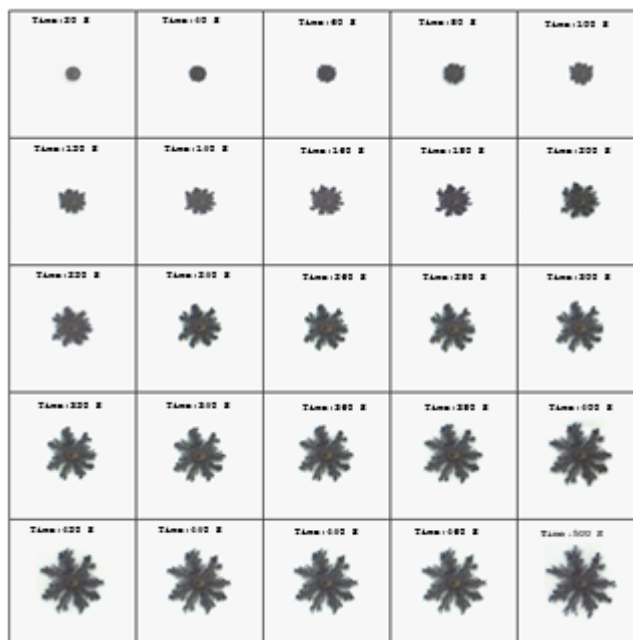
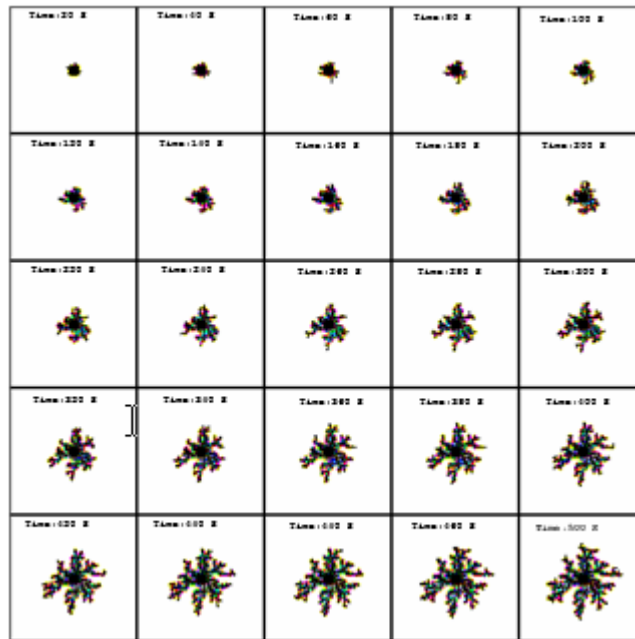


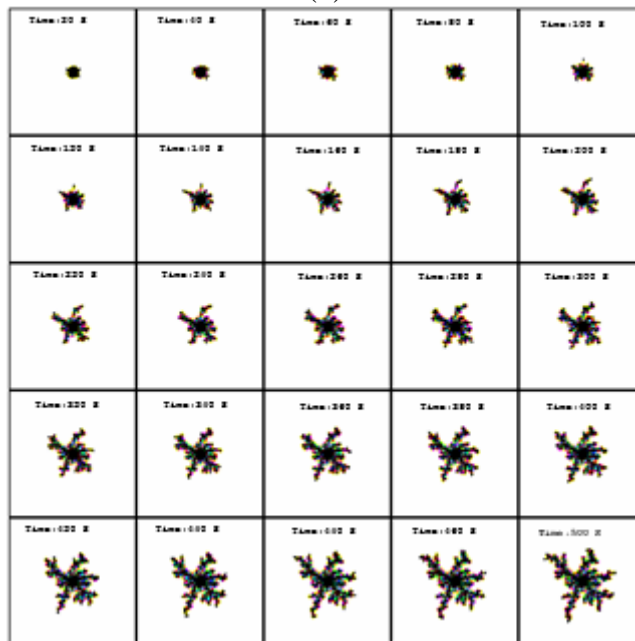
Fig. 5. Locations of the thermocouples at the bottom of the electrochemical cell



(a)

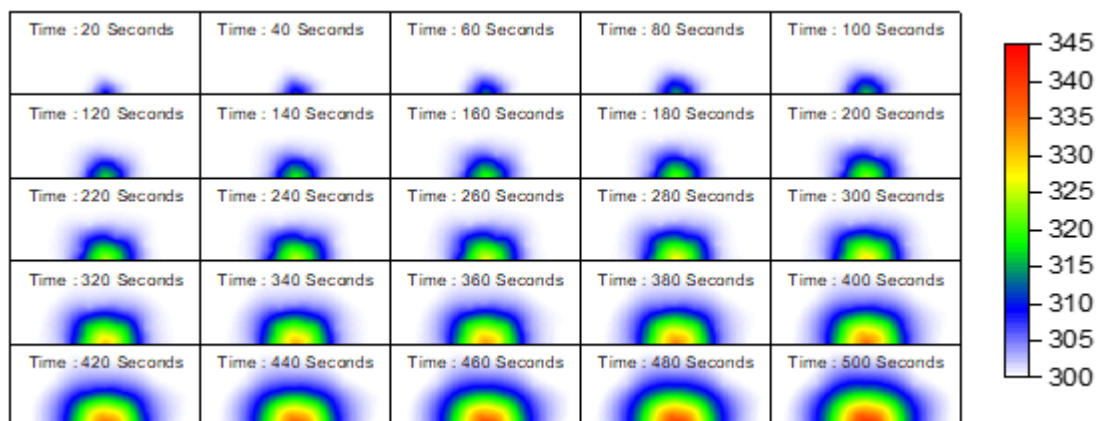


(b)

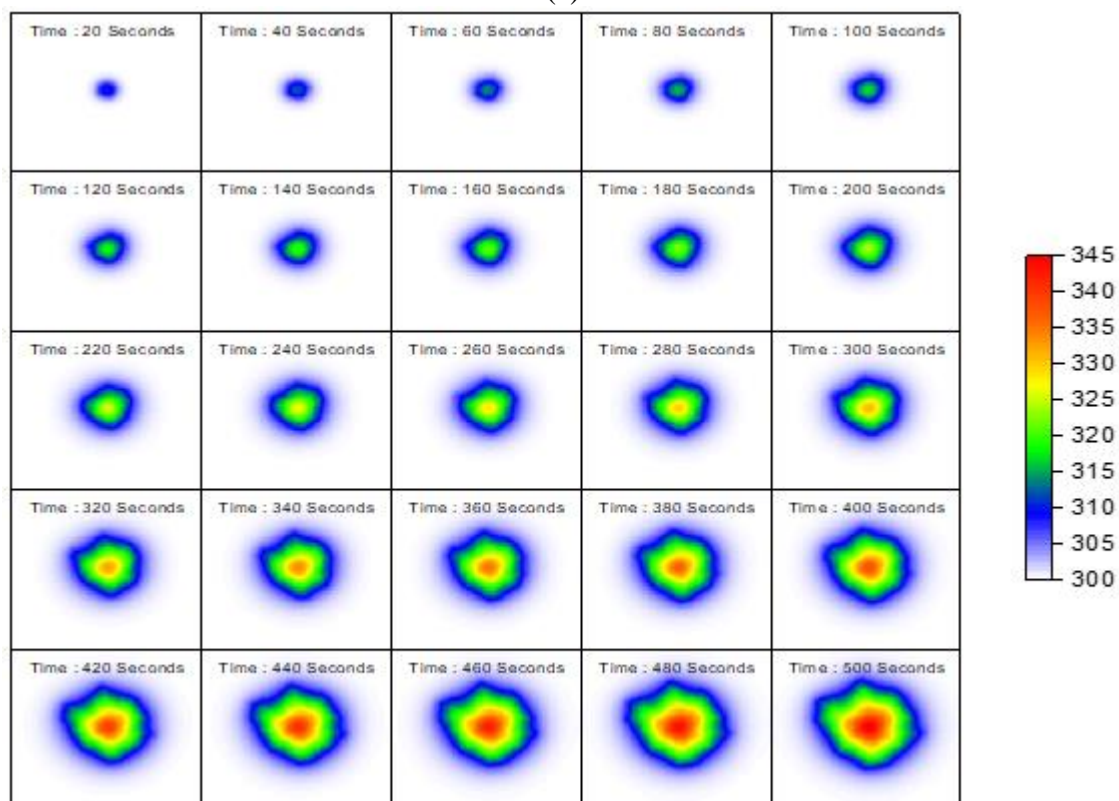


(c)

Fig. 6. First 500secs experimental vs. simulated images of the deposited zinc of 0.2N electrolyte at applied voltage of 20V.
 (a): experimental, (b): nonisothermal simulation,(c): isothermal simulation.



(a)



(b)

Fig. 7. Experimental vs. simulated results of temperature contours of the deposited zinc of 0.2N electrolyte at applied voltage of 20V. a): experimental contours , b): simulated contours

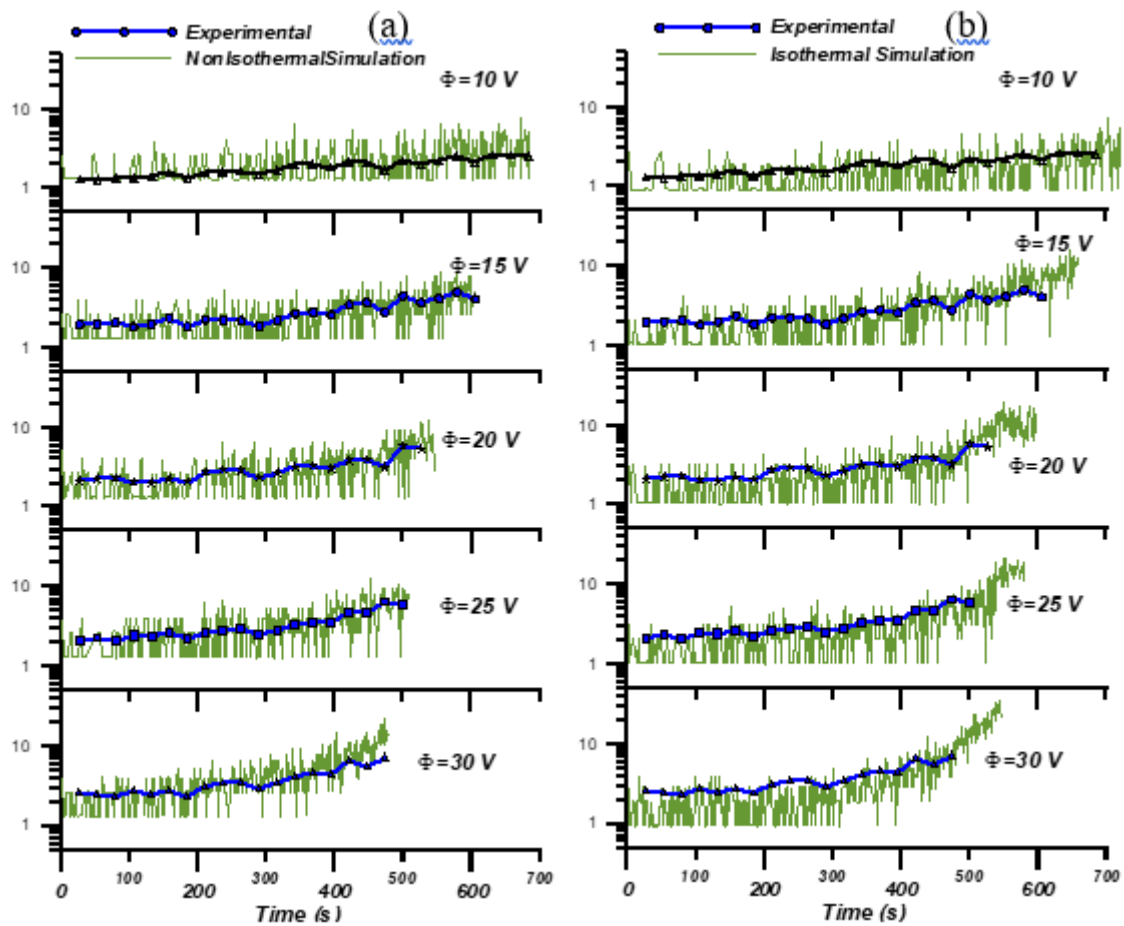


Fig. 8. Experimental vs. simulated results of deposition rate of Zinc at different value of applied voltage. (a): experimental vs. isothermal simulations. b) experimental vs. thermal simulations.

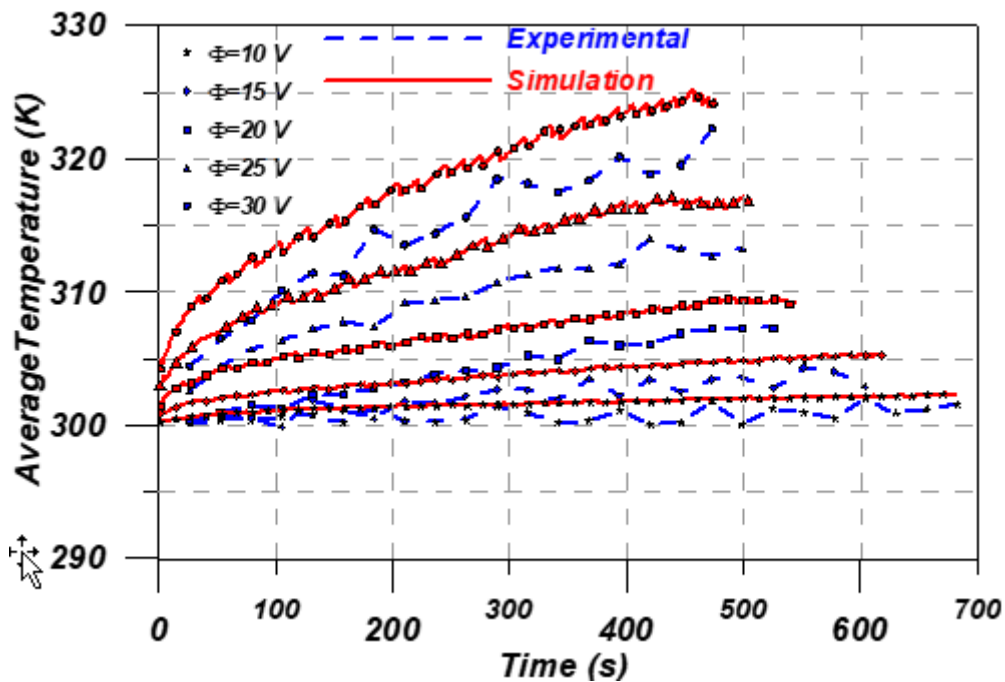


Fig. 9. Experimental vs. simulated results of average temperature of deposited Zinc at different values of applied voltage.

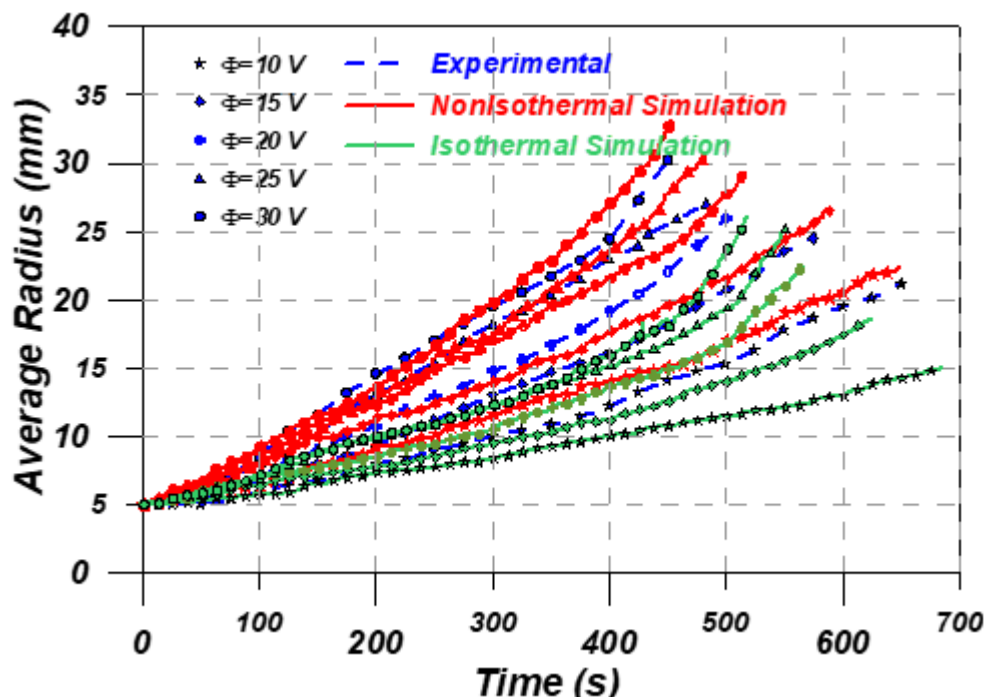


Fig. 10. Experimental vs. simulated results of average radius of deposited Zinc at different values of applied voltage.

REFERENCES

- Allen, M. P. and D. J. Tildesley, "Computer Simulation of Liquids", Oxford University, New York Press, 1990.
- Alkire, R. C. and R. D. Braatz, "Electrochemical Engineering in an Age of Discovery and Innovation", *AIChE J.*, Vol. 50, No. 9, 2000-2007, 2004.
- Alkire, R., "Processing Nanostructured Materials: The Need to Integrate Experimental Data with Multiscale Continuum/ Noncontinuum Simulation," *J. Electroanalytical Chemistry*, Vol. 559, pp. 3-12, 2003.
- Alkire, R., "Transient Behavior During Electrodeposition into a Metal Strip of High Ohmic Resistance", *J. Electrochem. Soc.*, Vol. 118, No. 12, pp. 1935, 1971
- Bockris, J. O'M and M. Enyo, "Mechanism of electrodeposition and dissolution processes of copper in aqueous solutions", *Trans. Faraday Soc.*, Vol. 58, pp. 1187, 1962.
- Drews, T. O., S. Krishnan, J. Alameda, D. Gannon, R. D. Braatz, and R. C. Alkire, "Multiscale Simulations of Copper Electrodeposition onto a Resistive Substrate", *IBM J. Res. & Dev.*, Vol. 49, No. 1, pp. 49-63, 2005.
- Gear, C. W., J. Li, and I. G. Kevrekidis, "The Gap-Tooth Method in Particle Simulations", *Phys. Lett. A*, Vol. 316, No. 3-4, 190-195, 2003.
- Gomer, R., "Diffusion of adsorbates on metal surfaces", *Rep. Prog. Phys.* Vol. 53, No. 7, pp. 917-1002, 1990.

Hansen, U., S. Rodgers, and K. F. Jensen, "Modeling of Metal Thin Film Growth: Linking Angstrom-Scale Molecular Dynamics Results to Mi-cron-Scale Film Topographies", *Phys. Rev. B*, Vol. 62, pp. 2869-2873, 2000.

Hillson, P. J., "The mechanism of the reaction at a Cu/Cu²⁺ electrode", *Trans. Faraday Soc.*, Vol.50,385-393,1954.

Ismail, A. E., G. C. Rutledge, and G. Stephanopoulos, "Multiresolution Analysis in Statistical Mechanics -I. Using Wavelets to Calculate Thermodynamic Properties," *J. Chem. Phys.*, Vol.118, No.10, 4414-4423, 2003.

Jingxian, Y., L. Wang, L. Su, X. Ai, and H. Yang, "Temperature Effects on the Electrodeposition of Zinc", *J. Electrochemical Soc.*, Vol.150, No.1, C19, 2003.

Kalos, M.H. and P. A. Witlock, "Monte Carlo Methods". Part I: Theory, John Wiley & Sons, New York, 1986.

Lopez, C. F., P. B. Moore, J. C. Shelley, M. Y. Shelley, and M. L. Klein, "Computer Simulation Studies of Biomembranes using a Coarse Grain Model", *Comp. Phys. Comm.*, Vol.147, No.1, pp.1-6, 2002.

Levi, A. C., and M. Kotrola, "Theory and simulation of crystal growth", *J. Phys. Condens. Matter.*, Vol.9, No.2, pp.299, 1997.

Mehl, W. and J. O'M. Bockris, "Mechanism of Electrolytic Silver Deposition and Dissolution", *J. Chem. Phys.* Vol.27, pp.818-819, 1957.

Matlosz, M., P. H. Vallotton, A. C. West, and D. Landolt, "Nonuniform Current Distribution and Thickness During Electrodeposition onto Resistive Substrates", *J. Electrochem. Soc.*, Vol.139, No.3, 752, 1992.

Ogata, Y., K. Yamakawa and S. Yoshizawa, "Current-time behavior for copper electrodeposition". I. Theoretical analysis based on a surface diffusion model" *J. Applied Electrochem*, Vol.12, No.4, pp.439-447, 1982.

Pricer, T. J., M. J. Kushner, and R. C. Alkire, "Monte Carlo Simulation of the Electrodeposition of Copper -II. Acid Sulfate Solution with Blocking Additive", *J. Electrochemical Soc.*, Vol.149, No.8, pp.306, 2002.

Rikvold, P. A.M, I.A. Hamad and G. Brown," Determination of the Basic Timescale in kinetic Monte Carlo Simulation by Comparison with Cyclic-Voltammetry Experiments", *Surface Science*, Vol.572, pp. 355, 2004.

Schroter, M. , K.Kassner, I. Rehberg, J. Claret, and F. Sagues, "Does Ohmic Heating Influence the Flow in Thin Layer Electrodeposition?", *Physical Review E*66,026307, 2002.

Slaiman Q. J. M. and W. J. Lorenz, "Investigations of the kinetics of Cu/Cu²⁺ electrode using the galvanostatic double pulse method", *Electrochimica. Acta*, Vol.19, pp.791-798, 1974.

Tor Hurlen, "A crystal-growth treatment of cathodic deposition of the iron-group metals", *Electrochimica Acta*, Vol.38,No.13,pp.1783-1786, 1993.

Tobias, C. and R. Wijsman, "Theory of the Effect of Electrode Resistance on Current Density Distribution in Electrolytic Cells", *J. Electrochem. Soc.* Vol.100,No.10,pp. 459,1953.

Vitanov, T., A. Popov, and E. Budevski, "Mechanism of Electro crystallization". *Electrochem. Soc.*, Vol.121,No.2, pp.207-212, 1974.

Vlachos, D. G.," Multiscale Integrations Hybrid Algorithms for homogeneous heterogeneous reactors", *AIChE J.*, Vol.43, No.11, pp.3031-3041, 1997.